5th International Conference on Experimental Fluid Mechanics – ICEFM 2018 Munich
Munich, Germany, July 2-4, 2018

Instantaneous 3D imaging of turbulent stratified methane/air flames using computed tomography of chemiluminescence

J Menser[1*], A Unterberger[1], A Kempf[1] and K Mohri[1]
[1]University of Duisburg-Essen, Institute for Combustion and Gas Dynamics – Fluid Dynamics, Duisburg, Germany
*jan.menser@uni-due.de

Abstract

The demand for cleaner combustion and reduction of NOx emissions calls for continued research on better understanding combustion processes, such as lean combustion using stratification. The computed tomography of chemiluminescence (CTC) technique, provided by Floyd (Floyd, Geipel et al. 2011, Floyd and Kempf 2011), was applied for the first time to the Cambridge stratified burner (Floyd and Geipel et al. 2011, Floyd and Kempf 2011), operated with the non-swirl conditions SwB1, SwB5 and SwB9. A large number of CCD cameras (number of views $N_q = 30$), were used to reconstruct the instantaneous and time-averaged chemiluminescence fields directly in 3D. The optimum camera locations and settings of the algorithm were chosen based on our previous CTC work on a swirl flame (Mohri, Goers et al. 2017). We compare the reconstructions with the Direct Numerical Simulation (DNS) data that Proch has recently published for the SwB1 case (Proch, Domingo et al. 2017, Proch, Domingo et al. 2017). The highly resolved DNS data, 10 px per mm shown in figure 4, was down-sampled and blurred, to match the reconstruction domain resolution of 4 px per mm, and the estimated image blurring based on the camera exposure time and the flame velocity from the DNS data. The flame structures in the reconstructed field show a very good qualitative agreement with the filtered DNS field, demonstrating the quality of CTC.

1 Introduction

The CTC (Floyd and Geipel et al. 2011, Floyd and Kempf 2011, Gordon 1974) is based on the algebraic reconstruction technique (ART) (Gordon 1974). Floyd and Kempf et al. (2011) first demonstrated high-resolution 3D reconstructions of the CH* chemiluminescence field for a CH_4 /O_2 matrix burner, consisting of 21 laminar diffusion jet flames, which exhibit multiple flame fronts, resolving structures of approximately 200 µm over a domain width of 22 mm. Floyd et. al (Floyd et al. 2011) then reconstructed the geometry of a premixed turbulent opposed jet flame using 10 views that were obtained from 5 cameras, which utilised mirrors to record two images per camera. Most recently, Mohri et al. (Mohri, Goers et al. 2017) reconstructed a highly turbulent swirl flame using 24 views, summarising the strengths and weaknesses of the CTC technique for examining a real turbulent flame and providing best practice on how to assess the reconstructions.

In this paper we present the first CTC reconstructions of the non-swirled Cambridge stratified flames, using the latest experimental setup that we designed for applications of the CTC (Mohri, Goers et al. 2017). The Cambridge stratified burner was designed as a test bench for inter-lab comparisons, and its highly complex flame structures serve as an ideal case for advanced applications of the CTC. The stratification strength is determined by dividing the equivalence ratio of the inner $\emptyset_i$ and outer $\emptyset_o$ flames, $SR = \emptyset_i/\emptyset_o$. SwB1 represents a fully premixed flame with $SR = 1$, and the SwB5 and SwB9 cases have increasingly higher stratification strengths, $SR = 2$ and $SR = 3$ respectively. Hence, higher stratifications transform the flame from a fully premixed state (SwB1) to a partially diffusion flame, with the fuel-rich region being in the centre. Several different flame conditions from the burner have been subject to various experimental and numerical investigations (Barlow, Dunn et al. 2012, Sweeney, Hochgreb et al. 2012, Proch and Kempf 2014, Proch, Domingo et al. 2017), but no instantaneous 3D flame geometry information has yet been provided from experiments.

2 Experimental setup

The burner (Sweeney 2012), illustrated schematically in Figure 1, consists of two ring slots surrounding a central bluff body. A premixed methane/air mixture emanates from each of the slots, with different levels of stratification depending on the equivalence ratios used, and both slots are encapsulated by an air coflow. The inner and outer cold flow velocities are constant in all cases, $v_i = 8.31$ m/s and $v_o = 18.7$ m/s respectively. Sixteen different operating conditions were first defined for this flame (Sweeney 2012). The non-swirled cases SwB1, SwB5 and SwB9, are defined in Table 1. The flow rates were controlled by Bronkhorst mass flow controllers, which were factory calibrated with an accuracy of +-1%. Visual inspection of the flow throughout the experiments showed the flow to be in a steady and continuous operation.

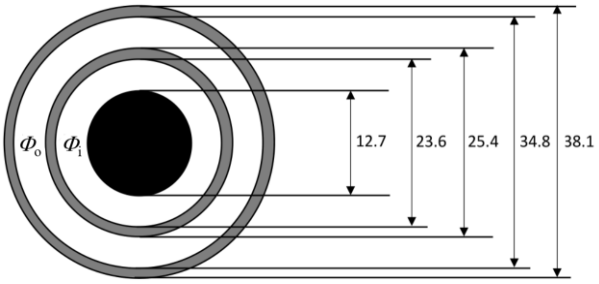

Figure 1: Dimensions of the Cambridge Stratified Swirl Burner.

The cameras were mounted on an aluminium plate, in which holes at predefined locations were machine drilled. The cameras were positioned with a precise angular spacing of 6° and a fixed distance of 400 mm to the flame centreline. Camera alignment was performed by taking images of a checkerboard target that was mounted on a rotation stage (from Thorlabs) at the flame location. The look-at direction of each camera was fine-tuned by turning the target by 6° each time, to face the camera orthogonally.

Table 1: Operating conditions of the flames, where ϕ is the equivalence ratio and SR is the stratification.

Case	**Outer flame**			**Inner flame**			**Coflow**		
	Air (slm)	CH_4 (slm)	ϕ_o	Air (slm)	CH_4 (slm)	ϕ_i	Air (slm)	$SR = \phi_i/\phi_o$	Power
SwB1	441.7	34.8	0.75	144.0	11.4	0.75	765.6	1	25.8 kW
SwB5	452.7	23.8	0.5	140.6	14.8	1.0	765.6	2	21.5 kW
SwB9	458.4	18.1	0.375	139.0	16.4	1.25	765.6	3	19.3 kW

The cameras used were Basler acA645–100 gm, featuring a ½" Sony ICX414 monochrome sensor with 659 by 494 pixels of size 9.9 µm × 9.9 µm. The peak spectral response of the cameras, at >60%, is between about 400 and 680 nm. Every second camera was equipped with a BG39 filter, to suppress the near infra-red emission from thermally excited H_2O. The remaining 15 cameras detected the chemiluminescence intensities in the visible range, including CH*, C_2* and CO_2*. Kowa C-mount lenses, with a focal length of 12 mm, were mounted on the cameras. To resolve finer structures, the camera exposure time was reduced to 300 µs but the CCD gain had to be increased significantly. The resulting increase in electronic shot noise became visible to the eye in the flame images. However, the CTC algorithm was capable of reconstructing a reasonable intensity field (*cf.* Figure 3).

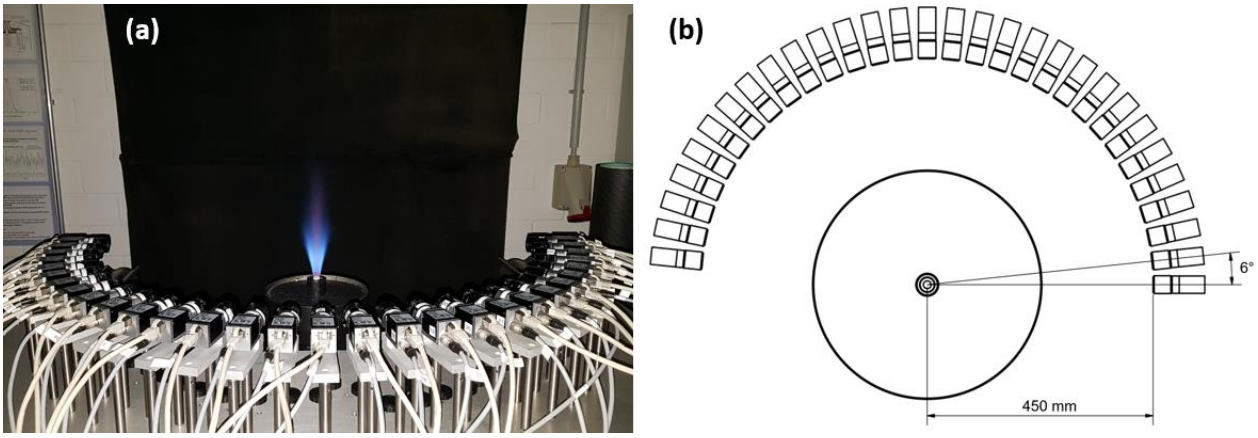

Figure 2: (a) The Cambridge stratified burner surrounded by the 30 CTC cameras. (b) top view schematic drawing of the setup.

3 Results and discussion

The 3D reconstructed instantaneous chemiluminescence fields for each flame are presented in Figure 3. The reconstructed field from flame images with water suppression filters was subtracted from the field without water suppression to recover the 3D field of the thermally excited H_2O, shown with a blue colour scale in Figure 3. The H_2O emission represents the hot products from combustion. The orange colour scale in Figure 3 illustrates the remaining chemiluminescence emission, which is clearly seen to envelope the H_2O field.

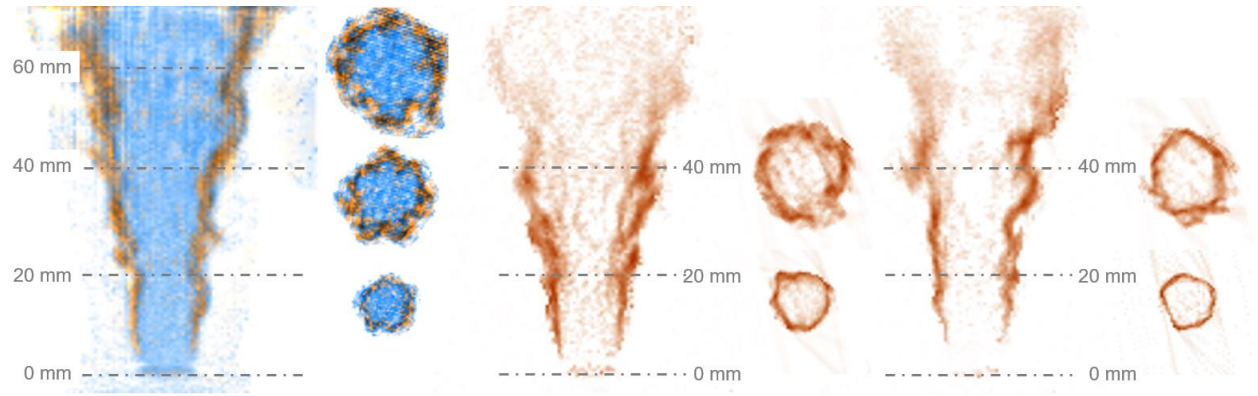

Figure 3: Horizontal and vertical slices from the 3D reconstructed Cambridge stratified flame for the Conditions SwB1 (left), SwB5 (middle) and SwB9 (right). The excited H_2O 3D field is shown in blue for the SwB1 case, and the remaining excited species chemiluminescence fields are shown in orange for all.

Generally, the flame shape is nearly similar for all the flames. This may be due in part to the constant cold inner and outer flow velocities. There is a distinct difference in the extent of the region occupied by the chemiluminescence emissions (without H_2O) between the fully premixed and stratified cases. For the SwB1 case, the region extends beyond the measurement height of approximately 70 mm, whilst it ends at a height above the burner of about 65 mm and 60 mm for the SwB5 and SwB9 flames respectively. Therefore, based on the above qualitative analysis, we note that the heat release zone surrounding the flame front is clearly influenced by the stratification.

Our comparison of the reconstructions with the independent DNS data for the SwB1 flame serve as a first validation for the reconstruction quality, which in its first phase is qualitative in nature. The biggest challenge in comparing our CTC reconstructions with DNS data is the significant difference in spatial and temporal resolution between the two data sets. The DNS field has a spatial resolution of 100 µm per voxel, whilst the CTC field is firstly temporally averaged by the exposure time of 300 µs, which corresponds to a

displacement of ~40 voxels in the DNS domain and results. Additionally, the spatial resolution of the reconstructed field is approximately four times lower than the DNS. Our approach to achieve a first meaningful comparison was firstly to blur the DNS field in the flame propagation direction by an estimated velocity displacement, and secondly to downsample the DNS field to match the reconstruction resolution. The resulting DNS field resembles the reconstructed field qualitatively, as shown in Figure 4, demonstrating that the reconstructions could resolve the flame shape well.

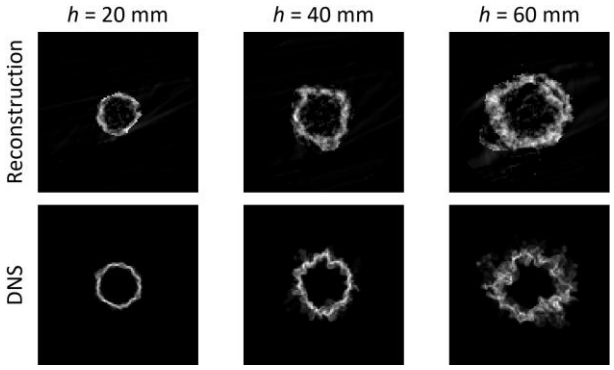

Figure 4: comparison of the horizontal slices at different heights above the burner h, from the reconstruction with the DNS field of similar temporal and spatial resolution.

Anurag (2016) have calculated the flame front curvature from the available DNS data of the SwB1 case, based on the method propose by Poinsot et al. (2005). We compare the flame curvatures calculated from the CTC data with those from the DNS. Due to the resolution discrepancies described earlier, the flame front is no longer a sharp (~1 – 2 mm) region in the reconstructions. Additionally, reconstructions are not absolutely free of artifacts, and also suffer from some electronic shot-noise carried through from the original flame images used for the reconstruction. To achieve a definable flame front signal, the tomographic reconstruction was filtered by a non-linear diffusion filter, which reduces background noise and enhances the high-intensity regions. The filtered volume was binarized by a threshold chosen to be 0.2 of the local peak intensity. Through morphological filtering (included in MATLAB, thin and shrink) the binarized volume was reduced to a 1 pixel thick surface, which is further assumed to represent the region surrounding the "flame front". It must be noted that the excited species chemiluminescence measurements used for the reconstructions excluded the H_2O contribution, but are not an absolute representation of the flame front due to presence of broadband emissions in addition to CH*. To determine the curvature, a circle or radius r was fitted to the deduced "flame front" region, and the curvature was calculated as $1/r$.

The curvatures calculated from the whole flame front region of the CTC field are compared to those from Anurag (2016). The two data sets exhibit a close agreement, especially for the peak and the overall shape of curvature variation.

5 Conclusion

In this work, the first instantaneous 3D reconstructions of the non-swirl Cambridge stratified flames were presented, and qualitatively validated with DNS data for the same flame case. The good agreement between the CTC and DNS data demonstrate the promising potential for CTC to provide reliable 3D flame shape information from low-cost and relatively simple to run experiments.

Acknowledgements

We gratefully acknowledge the funding by the Ministerium für Innovation, Wissenschaft und Forschung des Landes Nordrhein-Westfalen. Special thanks go to Prof. Simone Hochgreb for lending the Cambridge Stratified Burner to us for testing.

References

Anurag, K., "Effects of the choice of reaction progress variable definition on FSD transport and its modelling for LES." Master thesis, University of Duisburg Essen, Germany, 2017

Barlow, R. S., M. J. Dunn, M. S. Sweeney and S. Hochgreb (2012). "Effects of preferential transport in turbulent bluff-body-stabilized lean premixed CH4/air flames." Combustion and Flame **159**: 2563-2575.

Floyd, J., P. Geipel and A. M. Kempf (2011). "Computed Tomography of Chemiluminescence (CTC): Instantaneous 3D measurements and Phantom studies of a turbulent opposed jet flame." Combustion and Flame **158**(2): 376-391.

Floyd, J. and A. M. Kempf (2011). "Computed Tomography of Chemiluminescence (CTC): High resolution and instantaneous 3-D measurements of a Matrix burner." Proceedings of the Combustion Institute **33**(1): 751-758.

Gordon, R. (1974). "A tutorial on ART (Algebraic Reconstruction Technique)." IEEE Transactions on Nuclear Science **21**(3): 78 - 93.

Mohri, K., S. Goers, J. Schoeler, T. Dreier, C. Schulz and A. Kempf (2017). "Instantaneous 3D-imaging of highly turbulent flames using Computed Tomography of Chemiluminescence (CTC)." Appl. Opt **56**(26): 7385-7395.

Poinsot, T. and D. Veynante (2005). Theoretical and numerical combustion, RT Edwards, Inc.

Proch, F., P. Domingo, L. Vervisch and A. Kempf (2017). "Flame resolved simulation of a turbulent premixed bluff-body burner experiment. Part I: Analysis of he reaction zone dynamics with tabulated chemistry." Combustion and Flame **180**: 321-339.

Proch, F. and A. Kempf (2014). "Numerical analysis of the Cambridge stratified flame series using artificial thickened flame LES with tabulated premixed flame chemistry." Combustion and Flame **161**(10): 2627-2646.

Sweeney, M. S., S. Hochgreb, M. J. Dunn and R. S. Barlow (2012). "The structure of turbulent stratified and premixed methane/air flames I: Non-swirling flows." Combustion and Flame **159**: 2896-2911.